Nature and Science

Websites:
http://www.sciencepub.net/nature
http://www.sciencepub.net

Emails:
naturesciencej@gmail.com
editor@sciencepub.net

MARSLAND PRESS
Multidisciplinary Academic Journal Publisher

Role of high resolution CT and MRI in the assessment of painful ankle and foot

Emam Mohamed Abdelaziz, Hoda Mahmoud Abdelwahab, Mohamed Hasan Ateya*

Radiology Department, Faculty of Medicine, Al-Azhar University, Egypt
E-mail:Mohamedhasanzagg@gmail.com

Abstract: Background: Ankle pain is a common condition in adults that may cause significant discomfort and disability. A variety of soft tissue, osseous, and systemic disorders can cause pain. Emphasis in radiology has been directed toward advanced imaging, primarily computed tomography (CT), and magnetic resonance imaging (MRI), to an extent where radiographic findings may be overlooked or ignored. Multidetector CT is commonly used for the assessment of fractures and multiplanar reformation (MPR) has allowed accurate evaluation of fracture lines, dislocation and comminution for the selection of appropriate treatment. Magnetic resonance imaging (MRI) has become a frequently used adjunct in the evaluation of tendinous and ligamentous injures because it provides great detail of soft tissue structures through its multiplanar capability. **Aim of the Study:** to analyze the value of high resolution CT and MRI in patients with ankle and foot pain. **Patients and Methods:** this study will be performed on 159 patients presenting with ankle and foot pain There were 108 males and 51 females. The patients age range from 20 years to 69 years (mean age 44.5 years). The right ankle and foot was affected in 113 cases and the left side was affected in 29 cases. All cases were examined with either CT or MRI according to the clinical data obtained. CT examination was done to 52 patients, while MRI was done to 107 patients. **Results:** CT had high diagnostic accuracy at diagnosing fractures. At our study, 37% of patients had fractures while MRI had high accuracy at ligamentous and tendinous trauma. There were 34% of patients had tendinous injures and 23% of patients had ligamentous injures. **Conclusion:** CT has high sensitivity at accurate evaluation of fracture lines, dislocation and comminution that was not detected by plain radiography. Magnetic resonance imaging (MRI) has sensitivity and specificity at detection of soft tissue abnormalities including tendon, ligamentous injures, infectious and metabolic causes.

[Emam Mohamed Abdelaziz, Hoda Mahmoud Abdelwahab, Mohamed Hasan Ateya. **Role of high resolution CT and MRI in the assessment of painful ankle and foot.** *Nat Sci* 2019;17(12):284-298]. ISSN 1545-0740 (print); ISSN 2375-7167 (online). http://www.sciencepub.net/nature. 34. doi:10.7537/marsnsj171219.34.

Keywords: Achilles, fracture, impingement, Lateral Collateral, osteochondral defect, Peroneal, sprain, spur, tear, tenosynovitis, trauma.

Introduction

Ankle and Foot pain is a frequent symptom in patients with foot and ankle disorders. This complaint may cause significant disability and interfere with routine activities. Clinical diagnosis of the cause of pain is often difficult due to the broad spectrum of potential causes [1].

A variety of soft tissue, osseous, and systemic disorders can cause ankle and foot pain. Narrowing the differential diagnosis begins with a history and physical examination of the lower extremity to pinpoint the anatomic origin of the heel pain [2].

Fractures are more likely to occur in athletes who participate in sports that require running and jumping. Patients with ankle and foot pain accompanied by tingling, burning, or numbness may have tarsal tunnel syndrome [3].

Multidetector CT is commonly used for the assessment of calcaneal fractures, and multiplanar reformation (MPR) has allowed accurate evaluation of fracture lines dislocation, and comminution for the selection of appropriate treatment. Not surprisingly, anatomic and fracture detail obtained with multidetector CT has generated new approaches for the evaluation of calcaneal injury [4].

Magnetic resonance imaging (MRI) has become a frequently used adjunct in the evaluation of ankle and foot pain because it provides great detail of soft tissue structures through its multiplanar capability. Fascial thickening and increased signal intensity within the plantar fascia are typical MRI findings seen with plantar fasciitis. Admittedly, these findings are nonspecific, making MRI most useful for excluding other causes of heel pain. It has been shown that plantar fibromatosis, tumors, infection, and nerve entrapment are all reliably diagnosed with MRI [5].

Tendinous and Ligamentous injury caused by excessive range of motion at the joint in the absence of fracture or dislocation is called a sprain. Ankle sprain is common and accounts for >90% of ankle injuries

sustained in football, hockey, basketball, martial arts, and indoor volleyball. Recurrent injury can result in chronic instability and disability. MRI has multiplanar capability and superior soft tissue contrast, it is the tool of choice to evaluate the extent of ligament injuries in ankle sprain. It helps differentiate ligament injuries from other causes of ankle pain such as fracture, osteochondral injury, and tendon injury [6].

Results

This study included 159 patients, 108 males (68%) & 51 females (32 %), suffered from ankle and foot pain, most of them with established clinical diagnosis. The patients age range from 20 years to 69 years (mean age 44.5 years). Regarding history of trauma, there were 126 patients (79%) present with history of trauma and 33 patients (21%) represent no history of trauma. All cases were examined with either CT or MRI according to the clinical data obtained. CT examination was done to 52 patients (33%) while MRI was done to 107 patients (67%). Right ankle and foot was the site of complain at 113 patients (71%) and left side was affected at 46 patients (29%). The fractures of the distal end of the tibia and fibula were involved in twenty seven (27) cases, CT was done to twenty three (23) of them and MRI showed the fracture at four (4) cases. CT showed calcaneal fracture at nineteen (19) cases and one case on MRI. Talus was fractured at 6 cases four of them done CT and 2 of them done MRI.

The tendinous trauma were involved at 55 patients, the Achilles tendon was involved at twenty five (25) patients. Peroneal tendons were involved at twelve (12) patients. Tibialis anterior tendon was involved at three (3) patients. Tibialis posterior tendons were involved at seven (7) patients. Tendons were involved at eight (8) patients. The ligamentous injuries were involved at 36patients, the Lateral Collateral Ligament was involved at twenty one (21) patients, the Anterior talofibular was affected at 16 patients and the Posterior talofibular was involved at 5 patients. The Medial collateral ligament was involved at fifteen (15) patients. Anterior tibiotalar was involved at two (2) patients and Posterior tibiotalar was involved at seven (13) patients.

Diabetic foot was involved at four (4) patients detected by MRI. Talarosteochondral defect (OCD) was involved at eleven cases, eight of them diagnosed by MRI and three (3) patients diagnosed by CT. Stieda Process that can lead to posterior ankle impingement was detected at seven cases, five of them diagnosed by MRI and 2 of them diagnosed by CT. MRI diagnosed five cases of Haglund syndrome and four patients with Tarsal tunnel syndrome. Calcaneal spur was involved at eleven cases, seven of them were involved at CT and 4 were diagnosed from MRI. Planter fascitis was diagnosed at two MRI cases. Ostrigonium was involved at two (2) patients at CT and involved at one (1) patient at MRI. Osfibulare was involved at two (2) patients diagnosed by CT scan.

Osseous traumatic lesions

CT was done to diagnose cases of trauma with susceptible fracture at lower end of tibia and fibula or at calcaneus, tarsal bones and foot bones. CT scans taken in the transverse and sagittal planes should be combined with 3D CT reconstruction in order to get an accurate anatomical picture [7].

Pilon Fracture

Pilon fracture is any fracture through tibial plafond that encompasses wide spectrum of injury varying from low energy rotational injury to those caused by high energy trauma resulting from fall from height or motor vehicle accident. These fractures have frequently significant degree of metaphyseal or intra-articular involvement with varying amount of extension into shaft of tibia and often are open fracture or associated with severe soft tissue injury [8].

MRI may yield additional information about syndesmotic ligaments, tendons and osteochondral lesions, although it is used only exceptionally [7].

Ankle Dislocation

High-energy forces transmitted through the ankle, can fracture the malleoli. These injuries can result in failure of the mortise and supportive soft tissues, destabilizing the talus. With the ankle in plantar flexion, the joint is not stable, and translational forces can dislocate the talus from its mortise [9].

It is most frequently occur in young males and are caused by high-energy trauma during motor vehicle accidents, sports trauma, or falls. Low energy, rotational ankle fracture dislocations have been less frequently reported [10].

Posterior ankle dislocations are most common. These injuries occur when a high energy axial force drives the inverted foot backwards, trapping the wider anterior talus behind the tibial plafond. These injuries are commonly accompanied by syndesmotic failure or fracture of the lateral malleolus. This dislocation can potentially compromise the posterior tibial neurovascular structures [11].

Calcaneal fractures

It also known as Lover's fracture and Don Juan fracture, is a fracture of the calcaneus. It is usually caused by a fall from height [12].

The calcaneus is the most commonly fractured bone of the tarsi and represents 1-2% of all fractures. It articulates with the talus through the subtalar joint complex [13].

Plain radiographs are not able to provide all this information. Therefore, CT scans have become the criterion standard for the evaluation of complex fracture pathology. The 3-dimensional (3D) reconstruction of CT scans was proposed to improve

accuracy and precision of the evaluation of fracture pathology [14].

Fracture characterization is essential to guide the management of these injuries. Calcaneal fractures have characteristic appearances based on the mechanism of injury and are divided into two major groups, intraarticular and extraarticular. Most calcaneal fractures (70%–75%) are intraarticular and result from axial loading that produces shear and compression fracture lines [15].

The items "number of fragments" "fracture of the medial facet," "fracture line extending into the calcaneo-cuboid joint" and "concomitant injuries" a significant "improvement" was found after 3D CT presentation [14].

The Sanders classification relies on sagittally reconstructed CT images reformatted parallel and perpendicular to the posterior facet of the subtalar joint. Type I fractures are non-displaced. Type II fractures (two articular pieces) involve the posterior facet and are subdivided into types A, B, and C, depending on the medial or lateral location of the fracture line (more medial fractures are harder to visualize and reduce intraoperatively). Type III fractures (three articular pieces) include an additional depressed middle fragment and are subdivided into types AB, AC, and BC, depending on the position and location of the fracture lines. Type IV fractures (four or more articular fragments) are highly comminuted (Fig 11). The Sanders classification has been shown to have good inter-observer variability, making it useful in clinical practice [15].

Calcaneal stress fracture

The calcaneus is the second most common site of fatigue stress fractures, after the metatarsal bones. Insufficiency stress fractures may be seen in patients with rheumatoid arthritis or neurologic disorders. Stress fractures generally involve the posterosuperior or posterior aspects of the calcaneus and are usually oriented vertically or perpendicular to the long axis of the calcaneus. Patients with diabetes mellitus are at increased risk of calcaneal insufficiency fractures, particularly those involving avulsion of the posterior process of the calcaneus [16].

Talar Fractures

Fractures of the talus are uncommon. The integrity of the talus is critical to normal function of the ankle, subtalar, and transverse tarsal joints. Injuries to the head, neck, or body of the talus can interfere with normal coupled motion of these joints and result in permanent pain, loss of motion, and deformity [17].

Osteochondral fractures of the talar dome

Osteochondral lesions (OCL) of the talus involve both articular cartilage and subchondral bone of the talar dome. This term refers to a wide spectrum of pathologies including subchondral contusion, osteochondritisdissecans, osteochondral fracture and osteoarthritis resulting from longstanding disease. Subchondral bone involvement can be manifested by bone marrow edema, fracture, sclerosis and/or cyst formation. Cartilage damage may have a variable imaging appearance ranging from a small fissure, a distinct defect, flap formation or delamination [18].

Useful MR scoring parameters include lesion location, lesion size in 3 planes, subchondral bone marrow edema, subchondral cyst formation and/or sclerosis, status of the overlying cartilage, contour depression of the articular bone plate [19].

The Signal intensity of the fragment itself is also significant. Low signal intensity with all pulse sequences indicates necrosis, whereas hyperintensity on T1 weighted images indicates viable bone marrow. Viability can be further assessed by means of intravenous injection of gadolinium based contrast material with fat suppressed, TI weighted pulse sequences. Enhancement of the bone marrow of the fragment indicates viable tissue, whereas lack of enhancement indicates non-viable tissue [20].

Subtalar dislocation

Subtalar dislocation usually caused by an indirect high energy torsional force. Falls from a height or traffic accidents are the most common causes [21].

Subtalar dislocations can be sub-divided into medial, lateral, and anterior or posterior dislocations depending on the position of the calcaneus relative to the talus. The most frequent subtalar dislocation is the medial dislocation (80%). Lateral dislocations account for 17% and anterior or posterior dislocations are rare (3%) [21].

Cuboid fracture

Fracture of the cuboid results in loss of the lateral column support and this in turn would result in excessive valgus displacement of the medial column and forefoot and may cause medial soft tissue distraction type injuries such as the commonly associated posterior tibialtears [22].

CT scan and MRI can also show the cuboid fracture even at early stages; however in limping child the physician should be alert about possible small foot bones fractures and make sure to request appropriate MRI or CT projections [22].

Navicular fractures

The navicular is the keystone of the medial longitudinal arch, and is rigidly stabilized by an extensive network of dorsal and plantar ligaments. The rarity of this injury can be attributed to this surrounding rigid bony and ligamentous support. The navicular usually undergoes fracture and dislocation rather than pure dislocation [4].

Metatarsal shaft fractures

Metatarsal shaft fractures most commonly occur as a result of twisting injuries of the foot with a static

forefoot, or by excessive axial loading, falls from height, or direct trauma. Most patients with acute metatarsal fractures report symptoms of focal pain, swelling, and difficulty bearing weight [24].

Proximal fifth metatarsal Fracture

The blood supply to the proximal fifth metatarsal is important in understanding troublesome fracture healing in this area. it arises from three possible sources; the nutrient artery, the metaphyseal perforators, and the periosteal arteries. A watershed area exists between the supply of the nutrient artery and the metaphyseal perforators which corresponds to the area of poor fracture healing in the clinical setting [25].

The most frequent fracture seen is the fifth metatarsal, accounting for 68% of metatarsal fractures. Proximal fifth metatarsal fractures are divided into three zones. Zone one, zone two and zone three fractures account for 93%, four percent and three percent of proximal fifth metatarsal fractures, respectively [25].

Tendinous injures

They are entirely enclosed by an outer sheath called the paratenon, which also can respond to local mechanical conditions. In areas of high friction (e.g., behind the medial malleolus). The paratenon is a well-defined. double-layered synovial sheath as seen in the posterior tibial tendon. In areas of low shear (e.g., Achilles tendon), it is a thin layer of loose connective tissue [26].

The spectrum of abnormalities in tendons can be divided into Paratenonitis (tenosynovitis) which is seen as a significant amount of fluid in the tendon sheath. Tendinosis which is seen on MR images as tendon thickening with either normal signal intensity or heterogeneously increased signal intensity on both TI- and T2-weighted images. Or Partial tears occur in areas of underlying tendinosis that appear on MR images as the tendon shows increased thickness with linear and/or heterogeneous increased intrasubstance signal intensity on all sequences but the Complete tendon rupture is revealed as tendon gap and an empty tendon sheath frequently filled with fluid [26].

Achilles tendon

Achilles tendon rupture is the most common tendon rupture of the lower extremity, Although it is the strongest tendon in the human body [27].

There is an vascular zone about 2-6 cm from the base of the calcaneus and that this area of a vascularity is the most common site for rupture of the achillestendon [28].

Tendon injures occurs suddenly during movements that stress the Achilles tendon, such as running. The Achilles tendon is especially vulnerable to quick movements that place extreme stress on it [29].

Systemic diseases, such as rheumatoid arthritis, gout, lupus, and diabetes mellitus as well as fluoroquinolone use have also been implicated in tears of the Achilles. Chronic corticosteroid use is one of the predisposing factors particularly in elderly patients [30]. Achilles peritendinitis MRI shows T1WI show replacement of the normal high signal intensity fat and high T2 signal intensity around the tendon, which is partially circumferential and is most evident along the posterior surface of the tendon [4].

Partial tears show heterogeneous high signal intensity on fluid-sensitive MRI sequences, and there is incomplete interruption of the tendon fibers (Fig. 2). Involved fibers can partially retract and display a frayed or corkscrew appearance. Intratendinous or peritendinous edema and hemorrhage are often present in the acute setting [30].

A complete tear shows discontinuity of fibers while a partial tear shows tendon thickening and increased signal on T2-weighted images [27].

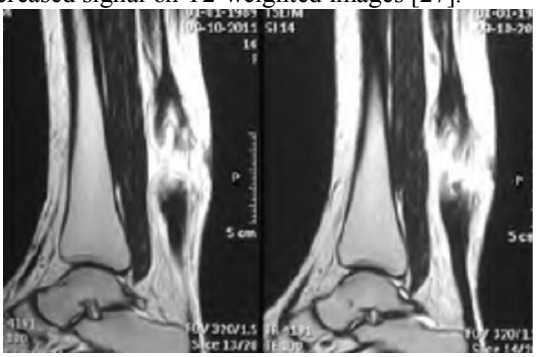

Figure (1) Sagittal T2WI show full thickness tear of the right Achilles tendon in a 31 year old man. There's complete disruption of continuity of the tendon, with retraction of its ends and an abnormal gap about 5 cm. The gap is filled with hematoma. There's also noted edema and fluid collection within the surrounding tissues. The tear is close to the tendon insertion [27].

Peroneal tendons

The intimate relationship of the superior peroneal retinaculum (SPR) with the peroneal tendons contributes to frequent concomitant diseases. Chronic insufficiency or tear of the SPR allows the peroneal tendons to dislocate out of the fibular groove and predisposes to peroneal tendon tears. Therefore, recognition of SPR injuries is important in guiding treatment options [32].

When there is expected injury to the plantar aspect of the PL tendon, additional MR imaging sequences should be performed in plane with the long and short axes of this tendon, with the long-axis plane paralleling the long-axis plane of the metatarsal bones (Fig 13) [33].

These include peronealtendinosis, tenosynovitis, partial-thickness and longitudinal full-thickness split

tears, tendon ruptures, peronealretinacular injuries, lateral ankle instability with tendon subluxations or dislocations from the retromalleolar groove and associated superior peroneal retinaculum (SPR) injuries, and intrasheath subluxation of the peroneal tendons within the retromalleolar groove [34].

Partial or split tears in the middle portion of the PLT often occur in the presence of a hypertrophied peroneal tubercle**.** Complete tears are more frequently found at the fibroosseous tunnel of the cuboid notch, where the PLT is deflected to the plantar area [35].

Several anatomic variants, including a flat or convex fibular retromalleolar groove, hypertrophy of the peroneal tubercle at the lateral aspect of the calcaneus, an accessory peroneus quartus muscle, a low-lying peroneus brevis muscle belly, and an osperoneum, may predispose to peroneal tendon injuries [33].

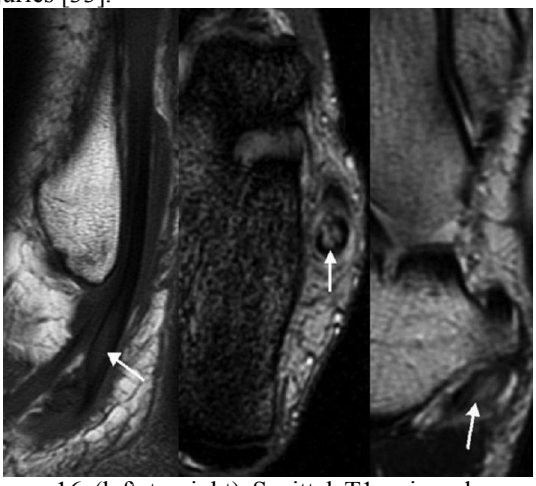

Figure 16 (left to right) Sagittal T1 spin echo, axial T2* and coronal T2 images. Longitudinal incomplete tear of the peroneus longus tendon (arrows) in the presence of a large peronealtubercle**.**

Increased signal intensity is associated with tendon disease but may also be due to the magic angle effect (Fig 13). Technical pitfalls, including those related to the magic angle effect, should not be misinterpreted as disease. The magic angle effect occurs when a structure is oriented at 55º relative to the static magnetic induction field (B0), which results in increased signal intensity in the structure on short echo time (<38msec) T1-weighted and proton-density–weighted MR images. Imaging with the foot in mild plantar flexion (approximately 20°) can help decrease the magic angle effect.

Tibialis anterior tendon

Ruptures of the tibialis anterior tendon are uncommon. They can generally be divided into two categories: first, acute rupture secondary to laceration, a sudden violent force, and fractures; and, second, acute-on-chronic or spontaneous rupture [36].

The common sites for tibialis anterior tendon rupture are its insertion into the adjacent surface of the medial cuneiform bone, beneath the oblique superomedial limb of the inferior extensor retinaculum [36].

A tendinous gap that is apparent at the site of a complete tear can be filled with fluid, fat, or scar tissue depending on the age of the tendon rupture [36].

Posterior tibial tendon

Decreased blood supply to the tendon also predisposes it to injury. This is described in the segments of the tendon behind and 1.5 cm distal to the medial malleolus. They may also occur at the navicular insertion site or 2-3 cm proximal to it [26].

In difficult clinical situations (e.g., acute trauma) and in early stages of posterior tibial tendon dysfunction. MR imaging is an important tool for establishing a diagnosis and initiating treatment to prevent secondary foot deformities [38].

Heterogeneity of the tendon signal and longitudinal tears (splits) as well as complete ruptures can be difficult to evaluate on sagittal images but can occasionally be detected (Fig. 4). This is due to the oblique course of the posterior tibial tendon and to the fact that such patients frequently have foot deformities [26].

FHL tendon disorders

The tendon is susceptible to injury anywhere along its course, since it traverses multiple fibro-osseous tunnels and undergoes a number of directional changes (between the talar tubercles, beneath the sustentaculumtali, at the decussation, and at the hallucalsesamoid tunnel). Tenosynovitis of the plantar FHL may occur alone or in association with tendinosis. Stenosing tenosynovitis at the intersesamoid fibro-osseous tunnel, although uncommon, may clinically masquerade as a tendon rupture [39].

Complete ruptures of the flexor hallucislongus (FHL) tendon are most commonly diagnosed in high-level athletes such as runners, ballet dancers and tennis players [40].

It is commonly thought that the master knot of Henry, the fibrous connection between the FHL and FDL, will prevent recoiling of one end of the tendon depending on the location of the rupture. If the rupture occurs proximal to the knot, the portion of tendon distally will be held in place by the fibrous connection. An injury distal to the knot would prevent contraction of the proximal end [41].

Ankle sprain and ligamentous injures

The ankle joint is supported by three groups of ligaments: lateral collateral ligaments, medial collateral ligaments, and the syndesmotic ligament complex. Ligaments that generally appear homogeneously hypointense on all imaging sequences

may include the ATFL, CFL, and superficial deltoid ligament. Other ankle ligaments may show a mixed or striated signal intensity pattern; these include the posterior talofibular ligament (PTFL), posterior tibiofibular ligament, and deep deltoid ligament [42].

The lateral collateral ligament complex includes the ATFL, PTFL, and CFL. The medial collateral ligament complex, also known as the deltoid ligament, consists of deep and superficial layers (Figure 4). The deep ligaments have talar attachment and cross one joint, and consist of anterior and posterior tibiotalar ligaments. The superficial ligaments have variable attachments and cross two joints. The three components of the superficial layer are the tibiocalcaneal ligament, tibionavicular ligament, and tibiospring ligament [6].

The syndesmotic ligaments consist of the AiTFL, PiTFL, inferior transverse tibiofibular ligament, and inferior interosseous ligament or membrane. These ligaments are best demonstrated on axial and coronal MRI with low to intermediate signal intensity [42].

The MRI characteristics of acute injuries to the ankle ligaments include morphological and signal intensity alterations within and around the ligaments**.** Morphological alterations may include abnormal thinning, thickening, irregularity, discontinuity, or detachment. Signal intensity alterations can be heterogeneous with increased intra-ligamentous signal intensity on fluid-sensitive MRI sequences, which indicate intra-ligamentous oedema or haemorrhage [43].

Other associated features include obliteration of the fat planes around the ligament, extravasation of joint fluid into the adjacent spaces, and bone marrow oedema or contusion. Acute ligamentous injuries are rarely treated surgically. Concomitant injuries such as fracture, osteochondral injury, or tendon injury are common [44].

A three-point MRI grading system is used to describe acute ankle ligament injuries. Grade I injury is defined as mild sprain with superficial soft tissue oedema around the ligament. Grade II injury is a partial thickness tear and is seen as thickening / oedema and internal signal alteration within the substance of the ligament on MRI. Grade III injury is a complete tear, and MRI shows complete disruption or avulsion of the ligament [45].

The MRI manifestations of chronic ligamentous tear of ankle ligaments may be similar to acute injuries, which could be thickening, thinning, or irregular appearance of the ligaments. Nonetheless, there is usually no residual soft tissue oedema or haemorrhage. Scarring or synovial proliferation may be encountered surrounding the ligaments with decreased signal intensity in all pulse sequences [46].

Lateral ankle sprains represent 16% to 21% of all sports related traumatic lesions, and typically occur during forced plantar flexion and inversion.18 The ATFL is the weakest ligament and therefore the most frequently torn (Figure 6). The lateral collateral ligamentous complex usually demonstrates a predictable pattern of injury depending on the severity of ankle inversion. The ATFL is injured first, followed by the CFL and then the PTFL (Figure 6). The ATFL is injured in 83% of cases, the CFL in 67%, and the PTFL in 34% [47]. **(Fallat, 1998).**

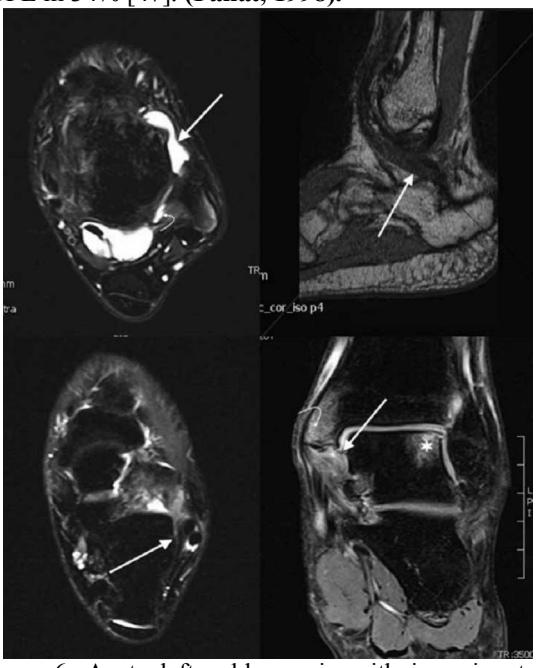

Figure 6. Acute left ankle sprain with inversion type injury in a 28-year-old man: (a) axial T2-weighted image with fat saturation showing complete absence of the anterior talofibular ligament (arrow). Partial tear of the posterior talofibular ligament at the talar attachment is also noted (curved arrow). Note the fluid at the anterolateral recess, ankle joint effusion, and fluid around the flexor hallucislongus tendon. (b) Sagittal turbo spin-echo proton density (PD)-weighted 3D SPACE showing thickened calcaneofibular ligament with intermediate signal intensity (arrow). (c) Axial T2-weighted image with fat saturation showing partial tearing of the calcaneo fibular ligament (arrow). (d) Coronal PD weighted image with fat saturation showing partial tear of the deep and superficial components of the deltoid ligament (arrow), associated bone mar row oedema (curved arrow) at the medial malleolus, and osteochondral defect at the talar dome (asterisk).

In chronic injuries of the ATFL, granulation and scar tissue may form within the anterolateral gutter, leading to impingement from entrapment of the synovial membrane between the anterior talus and the adjacent tibia or fibula [6].

Deltoid ligament complex injuries account for about 5% of ankle sprains. Pronation-eversion and extreme rotation are known to be the mechanism that leads to deltoid ligament injuries. Recent studies show deltoid ligament injuries may be more frequent than previously thought. Isolated deltoid ligament injuries are infrequent and often associated with lateral ligamentous injuries, syndesmotic injuries, or malleolar fractures particularly in Weber type B fracture [44].

The deep layer is more commonly injured than the superficial layer, and partial tears are more common than full-thickness tears. Sprains of the deep layer of the deltoid ligament are frequently noted on MRI in patients after inversion injuries (Figure 6) [46].

Syndesmotic ligament injury or high ankle sprain accounts for approximately 7% of ankle sprains. The mechanism of injury is thought to be forced external rotation with ankle dorsiflexion and pronation. The AiTFL is the most commonly torn ligament, and is almost always torn before the other syndesmotic ligaments [48].

The injuries can be either ligamentous tear, avulsion fracture, or both. They can be isolated or may occur in conjunction with other ankle ligamentous groups, or associated with Weber B or C ankle fractures. It is associated with a greater risk of chronic ankle dysfunction and persistent pain and usually requires a longer time to recover previous level of function, compared with other ankle sprains of similar severity that do not involve the syndesmosis [49].

Post-Traumatic Sinus Tarsi Syndrome

The sinus tarsi is a cone-shaped cavity in the lateral aspect of the midfoot between the anterosuperior aspect of the calcaneus and the inferior aspect of the talar neck. It opens laterally anterior to the lateral malleolus and terminates posteromedially behind the sustentaculumtali. The contents of the sinus tarsi include abundant fat surrounding vessels, nerves, and a ligamentous complex. The sinus tarsi ligaments, nerves, and vessels play an important role in the stabilisation and proprioception of the subtalar joint [50].

It is a common complication of ankle sprains; 70% of cases have a trauma history, and 30% have miscellaneous causes such as ganglion cysts, gout or pigmented villonodularsynovitis. Sinus tarsi syndrome is a clinical syndrome should not be established solely on MRI findings alone. It is characterized by persistent lateral ankle pain and hind foot instability [51].

In sinus tarsi syndrome, the T1-weighted hyperintense fat signal is replaced with a low signal on T1-weighted images due to fluid or scar tissue, and a bright signal on T2-weighed images, with disruption of or indistinct cervical and interosseous ligaments. Associated MRI findings include osteoarthritis of the subtalar joint with subchondraloedema or cysts of the talus or calcaneus, or contrast enhancement of the hypertrophied synovium [44].

Ankle impingement syndromes

They are painful conditions caused by the friction of joint tissues, which is both the cause and the effect of altered joint biomechanics. The leading causes of impingement lesions are posttraumatic ankle injuries, usually ankle sprains, resulting in chronic ankle pain [52].

The classification of these syndromes is anatomical based on their relationship with the talofibular joint; so they are classified in anterolateral, anterior, anteromedial, posteromedial, and posterior. In spite of that the damaging etiology can be similar in all of them, each location has a different symptom and clinical signs and specific findings in imaging studies [53].

Anterolateral Impingement Syndrome

The most common ankle injury is a sprain of the ATFL, which typically results from a plantar flexion/inversion mechanism A robust haemarthrosis and resultant synovitis can occur after injury. Over time, this can coalesce into a triangular or meniscoidhyalinized fibroid mass within the ALG [54].

Anterior Impingement (AI) syndrome

The AI is related to bone spurs in the tibial platform, typical of athletes that suffer a repeated forced dorsal flexion (dancers and football players) or repeated microtrauma [53].

Anteromedial impingement

Is an uncommon cause of chronic ankle pain that can be a result of a meniscoid lesion, which is represented by a soft tissue thickening anterior to the tibiotalar ligaments. The anteromedialmeniscoid lesion can appear isolated or arising from a partially torn deep deltoid ligament. [4].

Posterior ankle impingement syndrome (PAIS)

The anatomy of the posterior ankle is a key factor in the impingement syndrome. The secondary ossification nucleus is formed in the posterolateral aspect of the talus between 8 and 13 years of age and fusion with the rest of the talus in the first year after its formation. In 7% of the population there is a failure of this fusion, becoming the bone trigonum (ostrigonum). Other anomalies that can predispose to PI is a posterolateral prominent talar process (Stieda process), prominence of the posterior tibial malleolus and a protuberant posterior calcaneus process. The soft tissue lesion in the posterior aspect of the ankle can also cause PI: fibulotalar, intermalleolar and posteroinferiortibiofibular ligament, synovial sheath of the flexor pollicis and the posterior synovial recess of the tibiotalar and subtalar joints [53].

Evaluation with CT can visualize osseous variants, additional osseous bodies and osteochondral abnormalities and can be performed to assist with pre-operative management. MRI, with its superior soft-tissue contrast, plays an invaluable role in the evaluation of posterior ankle pain. One key feature is bone marrow edema (low T1 and high T2 signal) within the talus, calcaneus or an ostrigonum. Other features include increased signal at the synchondrosis, associated synovitis and thickening of the posterior ligaments, as well as the possibility of a posterior subtalar or tibiotalar ganglia being present [54]. ***(Berman et al., 2016).***

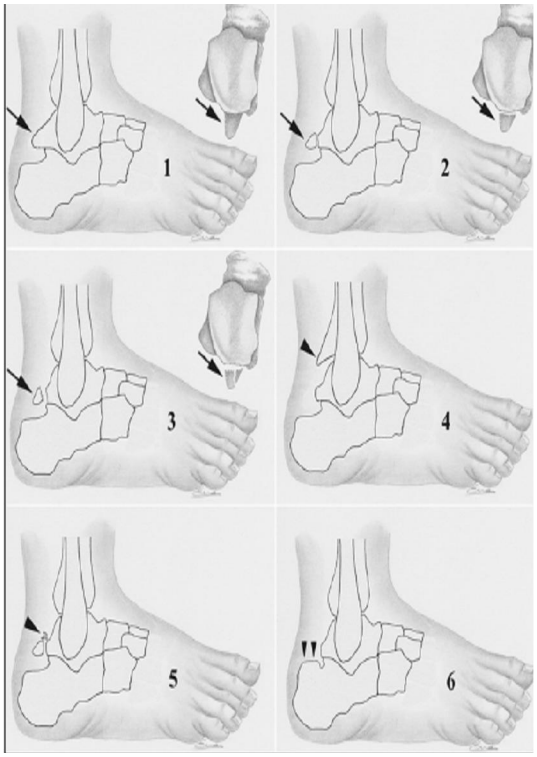

Fig…. Diagrams show (left image) osseous anatomic structures involved in posterior impingement: 1 = Stieda's process (arrows), 2 = ostrigonum (arrows), 3 = fractured lateral tubercle of talus (arrows), 4 = prominent down slope in posterior tibial articular surface (arrowhead), 5 = calcified inflammatory tissue (arrowhead), and 6 = prominent superior surface of calcaneal tuberosity (arrowheads). [52].

Miscellaneous conditions:

Retrocalcaneal Bursitis

Two bursae located near achilles tendon insertion. Superficial retroachilles Bursa, Located over achilles tendon, Irritated by constant rubbing by shoe and Associated with thin heel pad. Retrocalcaneal bursa, Located under achilles tendon, Irritated by calcaneus and Prominent posterosuperiorangle [55].

On MRI, a fluid collection between the posterior calcaneus and the insertion of the Achilles tendon can be seen, which shows low signal intensity on T1-weighted sequences and high signal intensity on T2-weighted and STIR sequences (Figs. 8B and 9). Enlargement of the normal bursal sac is the hallmark MRI finding, with values greater than 7 mm craniocaudal, 11 mm transverse, and 1 mm anteroposterior considered abnormal. Additionally, adjacent soft-tissue inflammatory changes are common [56]. ***(Lawrence D et al, 2013)***

Haglund Syndrome

It occurs commonly in adolescent girls who wear high heels with restrictive heel counters and may occur in people with rheumatoid arthritis. Haglund syndrome occur in patients who had a prominence of the posterosuperior surface of the calcaneus and wore tight, rigid shoe counters [57].

The condition is characterized by a prominent posterior bursal projection of the calcaneum, Achilles tendinosis, and inflammation of the retrocalcaneal and retro-Achilles bursae [58].

Plantar Fasciitis

Plantar fasciitis is the most common cause of inferior heel pain. Plantar fasciitis is most commonly due to repetitive mechanical stress, specifically, prolonged pronation stresses. This produces microtears and inflammation of the fascia and perifascial soft tissues. The condition is commonly seen in runners and obese patients [56].

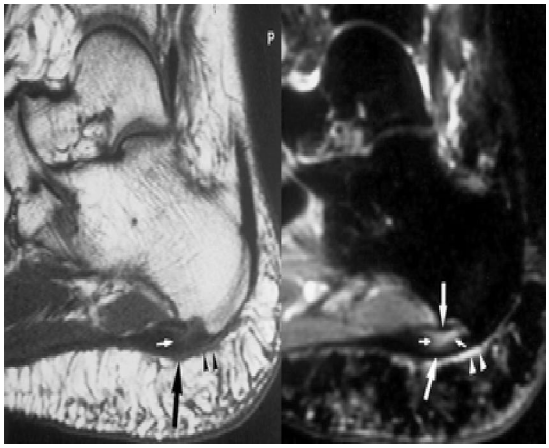

Fig (3-60): Plantar fasciitis. Sagittal T1-weighted (a) and STIR (b) MR images show marked thickening of the proximal plantar fascia (large arrows) with increased intrasubstance signal intensity (small arrows). Note also the perifascial edema, which has low signal intensity in (a) and high signal intensity in (b) (arrowheads)

Tarsal tunnel syndrome

The tarsal tunnel syndrome can be caused by extrinsic or intrinsic pressure on the posterior tibial nerve or on its terminal branches: the medial plantar

nerve, the lateral plantar nerve, the medial calcaneal nerve, the motor branch to the abductor muscle of the fifth toe and/or the inferior calcaneal nerve [59].

This syndrome can be idiopathic (in about 50% of cases) or associated with space occupying lesions including tumors, ganglion cysts from the subtalar joint or tendon sheaths, abnormal or accessory muscle (hypertrophic adductor halluces or accessory flexor digitorumlongus muscle, lipomas, varicose veins, trauma with bone spicule from an adjacent fracture, foreign bodies, iatrogenic causes such as calcaneal osteotomies with involuntary deep penetration medially, with fixation hardware or scar tissue [60].

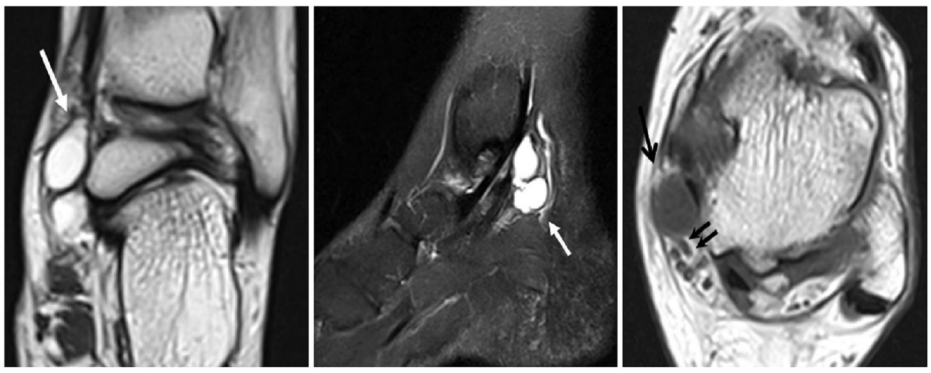

Fig. 6. Ganglion cyst. **(A)** Coronal T1-weighted and **(B)** sagittal fat-saturated T2-weighted MR images obtained at the tarsal tunnel level show a septated cystic lesion (white arrow in **A, B**) that was pathologically proven to be a ganglion cyst. **(C)** Axial T1-weighted image reveals a medial plantar nerve (double arrow) abutted by the ganglion cyst (single black arrow).

OsTrigonum Syndrome

The posterolateral talus has a variety of anatomic variants, including a normal tubercle; enlargement of the lateral tubercle of the posterior process of the talus, known as the "Stieda process"; and a separate ossicle, known as an "ostrigonum," which may or may not be fused to the posterior process of the talus. The mineralized ostrigonum appears between the ages of 7 and 13 years and usually fuses with the talus within 1 year. In approximately 10% of patients, it remains as a separate ossicle [56].

Clinically, the ostrigonum is asymptomatic unless impingement occurs; hence, ostrigonum syndrome is also known as "posterior ankle impingement syndrome." Other osseous abnormalities of the posterior talus may also result in posterior ankle impingement syndrome, such as the Steida process [52].

On MRI, ostrigonum syndrome shows abnormal signal intensity in the lateral talar tubercle, the ostrigonum, or both because of the bone impaction (Fig. 17). Furthermore, inflammatory changes will generally be present in the soft tissues of the posterior ankle, especially in the posterior synovial recess of the subtalar and tibiotalar joints [52].

Osteomyelitis

The calcaneus is a frequent location of osteomyelitis of the foot in both children and adults. In children, the disease more frequently results from hematogenous spread [61].

Computed tomography (CT) provides excellent definition of cortical bone and is superior to plain x-ray and MRI. Because of this, it is extremely useful in identifying sequestra, periosteal reaction, extent of bony erosion, and cortical destruction. CT also visualizes small foci of gas within the medullary canal, foreign bodies, soft tissue changes, and the full extent of sinus tracts [62]. CT is also superior to PR and MRI in the detection of subtle cortical erosions, foreign bodies, gas accumulation, small sequestra, and vascular/dystrophic calcifications.

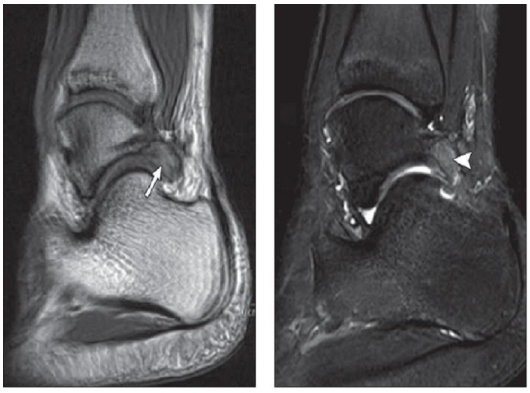

Fig. 17—18-year-old man with posterior ankle and heel pain. A and B, Sagittal T1-weighted image (A) and T2-weighted image with fat saturation (B) show ostrigonum (arrow, A) with bone marrow edema (arrowhead, B), consistent with ostrigonum syndrome.

Magnetic resonance imaging (MRI) is considered to be the imaging study of choice for the diagnosis and treatment of osteomyelitis. MRI is useful in detecting intraosseous and subperiosteal abscesses, provides clear anatomic detail, does not expose the patient to

ionizing radiation, and is rapidly completed and readily available in most centers. The addition of gadolinium contrast improves the result and gives better anatomic detail of soft tissue involvement [63].

Diabetic foot infections

Diabetic foot wounds consists of six grades: high-risk foot without ulcer (grade 0), superficial non-infected ulcer (grade 1), deep infected ulcer with limited cellulitis (grade 2), very deep infected ulcer with tendon/fascial and/or bone involvement (grade 3), limited gangrene (grade 4), or extensive gangrene and tissue necrosis (grade 5) [64]. Almost all diabetic foot infections are due to direct spread from a skin ulcer [65].

Although CT plays a limited role in the imaging of diabetes related foot complications, it has certain advantages over X-ray, such as the generation of images with high tissue contrast. Furthermore, it is more sensitive and specific for the identification of cortical erosions, small sequestra, soft tissue gas, calcifications, and foreign bodies compared with X-ray and MRI [66]. It has been recommended that MRI should be the first modality of choice in diabetic patients with soft tissue swelling without an apparent skin ulcer, followed by leukocyte-labeled scintigraphy [67].

Diabetes-related foot complications

Skin callus formation in atypical locations in the foot is a common problem in diabetic patients. In the forefoot, callus formation occurs beneath the first and fifth metatarsal heads and at the tip of the great toe. In the midfoot, callus formation occurs beneath the cuboid bone in patients with neuropathic disease and rocker bottom deformity (Fig. 1), and in the hind foot, most calluses develop at the heel [68].

On MRI, a skin callus appears as a focal infiltration or mass within subcutaneous fat, with low signal intensity on T1 weighted images and low to intermediate signal intensity on T2 weighted images. On MR images obtained after intravenous gadolinium injection, the callus might resemble a soft tissue infection [69].

Diabetic Ulcers typically appear as focal skin interruptions with elevated margins and associated soft tissue defects Unlike calluses, ulcers are detected as hyperintense areas on T2 weighted images, with intense peripheral enhancement on T1 weighted images, a finding indicative of granulation tissue at the base of the ulcer [66].

In patients with cellulitis but without apparent skin ulcers, CT can detect skin edema and subcutaneous fat stranding. Small collections within the diffusely infected soft tissue planes might be detected [70].

Abscess and sinus tract formation

On MRI, contrast enhancement along the wall of the fluid collection and a higher T2 signal intensity indicative of pus formation in comparison to the surrounding soft tissue edema are highly suggestive of an abscess. MRI also provides useful information about the localization and number of abscesses during the pre-surgical evaluation. The MRI features of a sinus tract resemble an abscess. Sinus tract may appear round if viewed in cross section and may be mistaken for an abscess. Therefore, sinus tracts should be evaluated in all imaging planes [66].

Necrotizing fasciitis, pyomyositis, and myonecrosis

The presence of air in soft tissues and fluid collections within the deep fascial planes indicate necrotizing fasciitis. This condition is characterized by thickening and enhancement of superficial and deep fascia, whereas subcutaneous fat tissues might be preserved [70].

Tenosynovitis

Septic tenosynovitis most commonly occurs in the peroneal and Achilles tendons, originating from lateral and calcaneal ulcers. Tendon thickening, hyperintensity on T2-weighted images, and enhancement around the tendon sheath are nonspecific findings, except in the presence of peritendinous enhancement coursing through an area of cellulitis and adjacent to an infected ulcer (Fig. 7) [71].

Osseous complications

Neuroarthropathy

Neuroarthropathy is an uncommon but severe complication of diabetic peripheral neuropathy [72].

Chronic repeated unperceived traumatic injuries to the joints of the foot results in Charcot neuroarthropathy. The diabetic patient is predisposed to this condition because of associated peripheral neuropathy and peripheral vascular disease [73].

There is progressive arthropathy characterized by cartilage damage, bone erosions, subchondral cysts, joint deformities and new bone formation. This usually affects the tarsometatarsal joints, causing collapse of the longitudinal arch and a ‘rocker-bottom’ deformity that increases load bearing on the cuboid [73].

Tumors And Tumor Like Lesions Of Soft Tissue And Bone

CT is a useful tool in differential diagnosis for diagnosing fatigue fractures, osteoarthritis or benign lesions such as osteoid osteoma. In soft-tissue tumors, it can help to assess secondary bone involvement in aggressive lesions [74]. Magnetic resonance (MR) imaging is the favored modality for evaluation of soft tissue tumors and tumor like conditions because of its superior soft tissue contrast, multiplanar imaging capability, and lack of radiation exposure. MR imaging is valuable for lesion detection, diagnosis, and staging [75].

Ganglion and synovial cysts are the most common soft tissue lesions in the ankle and foot region, most frequently located around the ankle or at the dorsum of the foot. Clinically, local pain, limited joint mobility or nerve entrapment (e.g. in the tarsal tunnel) may be present due to mass effect [76]. The MR features of ganglion and synovial cysts are those typical of cystic lesions (Fig. 4): hypo-intense or isointense to muscle on T1WI and homogeneous high signal intensity (SI) on T2WI. There is a faint rim enhancement of the cyst wall after gadolinium contrast medium administration. Typical cystic appearance can be altered in the case of hemorrhage or chronic inflammation, with higher SI on T1-WI and lower SI on T2WI, along with thickening and increased contrast enhancement of the cyst wall [77].

Plantar fibromatosis (Ledderhose disease) etiology is still a matter of debate, but it is thought to represent a benign fibroblastic tumor, rather than a pseudo tumor. Patients present clinically with fixed and subcutaneous nodules on the sole of the foot, along the course of the plantar aponeurosis. it is painful if inflamed or do compression on surroundings [78]. On both T1-WI and T2-WI the lesions are isointense or hypo-intense to skeletal muscle. Enhancement after IV gadolinium contrast medium administration is variable [77].

Morton's neuroma, (interdigital neuroma), most likely due to repetitive compression and irritation of the interdigital nerve. Therefore, the term Morton's fibroma is preferred [77]. Morton's fibromas are most commonly found in the second and third intermetatarsal spaces, and less frequently in the first and fourth. Also, more than one intermetatarsal space may be affected. Morton's fibroma is most commonly diagnosed in middle age, with a higher prevalence in women, and is believed to be related to the use of high-heeled shoes with increased weight bearing on the forefoot [79].

Morton's fibroma appears typically as a tear-shaped, spindle-shaped or dumbbell shaped lesion in the region of the neurovascular bundle on the plantar side of the deep intermetatarsal ligament (Fig...). Sagittal images reveal a widening of the interdigital nerve. Morton's fibromas display typical signal intensities on MR imaging sequences: isointense to muscle on T1WI and hypointense relative to fat tissue on T2WI [80].

Neurofibroma and schwannoma are relatively uncommon around the foot and ankle accounting for 5.4% and 3.9% respectively of all benign soft tissue lesions in this region. They most often occur in the 3rd and 4th decade and often present as slow growing painless lumps, though neurological symptoms may be present. The majority are isolated lesions, but multiple or plexiform lesions may be seen in neurofibromatosis type I [81].

Synovial osteochondromatosis is a disorder of the synovium resulting in metaplastic nodules of cartilaginous proliferation within joints, bursae or tendon sheaths which proceed to mineralize and detach. It is twice as common in men as in women and most often presents in the 3rd–5th decade. It is often mono-articular but may be bilateral. Malignant transformation into secondary synovial chondrosarcoma is rare [82]. In the late stage, CT may demonstrate numerous intra-articular mineralized bodies with secondary osteoarthritis. Earlier in the disease, non-mineralized intra-articular bodies present a more challenging diagnosis. In the initial proliferative phase, a lobulated intra-articular lesion is typical, with intermediate to slightly hyperintense signal on T1WI and high signal on T2WI (Fig. 9). Later, mineralized nodules may be seen as signal voids on all sequences, or as ossified bodies with a low signal cortex and central fatty marrow signal. Post contrast imaging shows enhancement of the hyperplastic synovium, more pronounced in the earlier stage [83].

Pigmented villonodularsynovitis (PVNS) is a benign proliferative intra-articular disorder of the synovium. Giant cell tumor (GCT) of the tendon sheath is the slightly more common extra-articular manifestation of the disorder which can affect bursae, tendons and ligaments [84]. PVNS does not generally contain mineralization but may be visible as dense effusions on plain radiographs. T1WI typically shows mixed intermediate to low signal soft tissue in the affected joint, depending on the relative proportion of fat, collagen and hemosiderin content (Fig. 7) The soft tissue mass demonstrates heterogeneous enhancement and there may be well-defined erosions and cysts with thin sclerotic margins on both sides of an affected joint [84].

Hemangioma may be superficial or deep and may be associated with fat, fibrous tissue and/or smooth muscle, often adapting their shape to adjacent structures. They account for 7% of benign soft tissue lesions in the foot and ankle. They most commonly present before 30 years of age and are often asymptomatic but may present with pain after exercise secondary to a local vascular steal phenomenon [77]. On MRI, vascular malformations may be well or poorly defined lesions with little mass effect for their size (Fig. 3). They may have high signal on T1WI, reflective of fat content or internal hemorrhage. The majority are slow flow lesions which appear T2 hyperintense and may demonstrate fluid-fluid levels. High flow lesions (arteriovenous malformations) demonstrate serpiginous flow-voids. Phleboliths may be seen as foci of low signal on all sequences. High

flow lesions generally demonstrate avid enhancement but may occasionally show delayed enhancement. The pattern of enhancement reflects the composition of the lesion and the flow characteristics of the involved vessel subtype. Atrophy in the adjacent muscle may be due to vascular steal and perilesional hemorrhage may also be present [85].

Rheumatoid nodules are granulomatous lesions with central areas of necrosis that occur in about 20% of patients with rheumatoid arthritis and less frequently in patients with rheumatic fever, systemic lupus erythematosus and ankylosing spondylitis [86]. MR imaging characteristics of rheumatoid nodules are non-specific (Fig. 10). They appear most commonly as ill defined nodular lesions isointense to muscle on T1WI with heterogeneous intermediate to high SI on T2WI. On contrast enhanced MR images, rheumatoid nodules display varying patterns of contrast enhancement, ranging from homogeneous enhancement in solid lesions with no central necrotic areas to heterogeneous increased SI or faint peripheral enhancement in nodules with less or more advanced central necrosis [87].

Synovial sarcoma is the most common malignant soft tissue tumor of the foot and ankle. Diagnosis is often delayed, with an average of 21 months between the onset of symptoms and the final diagnosis. The peak incidence of synovial sarcoma is observed in the second to fifth decade. Diagnosis is often challenging since synovial sarcoma can mimic other entities and clinical features are unspecific, with a slowly or rapidly growing, indolent or painful, firm and fixed mass. Risk of pulmonary metastases as well as lymphatic spread is high [88]. MRI is the imaging modality of choice to determine local extent of synovial sarcoma due to its superior contrast resolution. The tumor typically appears as a juxta-articular lobulated mass. Internal septa and multiple fluid-fluid levels may be seen. On T1-weighted MR images, the tumor is hypointense to subcutaneous fat. Signal intensity is similar to or slightly higher than that of muscle on T1-weighted images. The tumor is markedly heterogeneous on T2-weighted image and has been described as triple signal due to the presence of calcification (low signal), cellular component (intermediate signal), and haemorrhage / necrosis (high signal) [89].

Malignant Fibrous Histiocytoma occurs mostly in middle to late adulthood and occurs in the proximal region of the lower extremities.74 Undifferentiated pleomorphic sarcoma is usually low to intermediate signal intensity on T1-weighted sequences and intermediate to high on T2-weighted sequences. Myxoid UPS tends to be hyperintense on T2-weighted sequences due to the high water content of its lesions [90].

Myxoidliposarcomas lesions have low/intermediate T1 signal intensity due to the myxoidstroma and high water content of the myxomatous elements and very high T2 signal intensity. The presence and relative proportion of round cells may decrease the water content of the tumor, resulting in low to intermediate T2 signal. Most lesions demonstrate intense enhancement after administration of intravenous contrast. Encapsulated margins and thick internal septations are often visible [91].

Aneurysmal bone cysts (ABCs) account for 1% of primary bone tumors. They are more common in women than in men [92]. The lesion may arise as a primary lesion (65%) or secondary (35%) to pre-existing benign or malignant lesions (giant cell tumor, osteoblastoma, angioma, and frequently in the chondroblastoma of the calcaneus [93]. CT is useful to display the anatomical integrity of the lesion on the calcaneus. An ABC is usually seen as cortical erosion; however, in our case, no cortical erosion was seen on X-ray, but it was evident on the CT. The lesion density helps differentiate the cavity. Densities over 70 Hounsfield Units (HU) may represent solid lesions such as fibrous dysplasia. The image of blood and serum as a layer of fluid-fluid level is also defined as a feature of ABC. The densities of these layers vary between 16 and 47 HU [92].

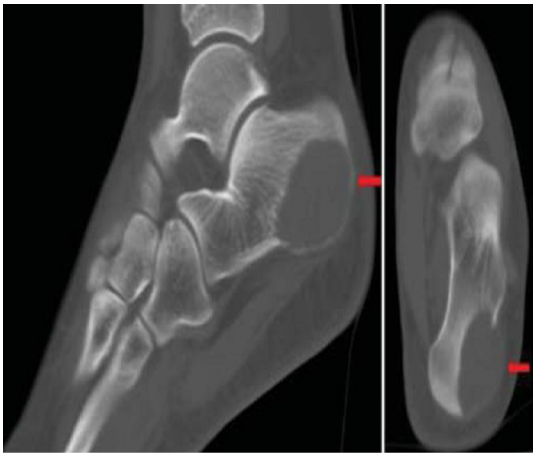

Figure 2: 17-year-old female with pain in the left heel diagnosed as due to an aneurysmal bone cyst. CT scans of the left foot (left) sagittal and right) coronal views show lytic mass lesion (arrow), 35 × 25 mm in dimension, localized postero-laterally, leading to cortical bone erosion, expansion, and destruction [94].

The MRI images of ABC on T1 and T2 typically show a non-homogenous cystic lesion and multiple fluid-fluid levels surrounded by a rim with low signal. The fluid-fluid levels are better evaluated on a T2W

MRI. Internal septae were also visualized better on MRI [92].

Fluid-fluid levels may also be seen in giant cell tumors, telangiectatic osteosarcomas, and chondroblastomas. The patient's age, localization of the lesion, and radiological images of the lesion can be of help in differential diagnosis [92].

References

1. Lemont H, Ammirati KM, Usen N. Plantar fasciitis: a degenerative process (fasciosis) without inflammation. J Am Podiatr Med Assoc. 2003; 93:234–7.
2. Love C, Din AS, Tomas MB, Kalapparambath TP, Palestro CJ: Radionuclide bone imaging: An illustrative review. Radiographics 23 (2): 341 – 358, 2003.
3. Berger FH, de Jonge MC, Maas M. Stress fractures in the lower extremity. The importance of increasing awareness amongst radiologists. Eur J Radiol 2007; 62:16.
4. Kenneth Badillo, Jose A. Pacheco, Samuel O. Padua. Multidetector CT Evaluation of Calcaneal Fractures. Published online 10.1148/rg. 311105036. RSNA, 2011.
5. Rosenbaum A, Di Preta J, and Misener D. Plantar Heel Pain. Division of Orthopaedic Surgery, Albany Medical College,2013.
6. Chu P, Chan W, Lee H, et al. Magnetic Resonance Imaging of Ligamentous Injuries in Ankle Sprain. Hong Kong J Radiol.2017;20:17-27.
7. Gardner MJ, Streubel PN, McCormick JJ, et al. Surgeon practices regarding operative treatment of posterior malleolus fractures. Foot Ankle Int. 2011;32:385-393.
8. Mishra N and Yadav P. Surgical treatment of Pilonfracture. IJOS 2017; 3(4): 16-22.
9. Southerland JT (ed). McGlamry's Comprehensive Textbook of Footand Ankle Surgery, 4th Edition. Lippincott Williams & Wilkins;2013.
10. Davenport M and Bailey RA. Ankle dislocation reduction. eMedicine. May 8, 2012.
11. Thangarajah T, Giotakis N and Matovu E. Bilateral ankle dislocation without malleolar fracture. J Foot Ankle Surg 2008;47:441-6.
12. Juliano P and Nguyen HV. Fractures of the calcaneus. OrthopClin North Am. Jan 2001; 32(1):35-51.
13. Baptista M, Rui Pinto R and Torres J. Radiological predictive factors for the outcome of surgically treated calcaneus fractures. ActaOrthop. Belg 2015; 81, 218-224.
14. Roll C, Schirmbeck J, Müller F, et al. Value of 3D Reconstructions of CT Scans for Calcaneal Fracture Assessment. Foot & Ankle International 2016; 37; (11); 1211-1217.
15. Daftary A, Haims A and Baumgaertner M. Fractures of the Calcaneus: A Review with Emphasis on CT. RadioGraphics 2005;25:1215-1226.
16. Lawrence D, Rolen M, AbiMorshed K, et al. MRI of Heel Pain (2013). AJR 2013;200:845–855.
17. Fortin P, and Balazsy J. Talus Fractures: Evaluation and Treatment. J Am Acad Orthop Surg 2001;9:114-127.
18. Posadzy M, Desimpel J and Vanhoenacker F. Staging of Osteochondral Lesions of the Talus: MRI and Cone Beam CT. Journal of the Belgian Society of Radiology 2017;101(S2):1-7.
19. Barr C, Bauer JS, Malfair D, et al. MR imaging of the ankle at 3 Tesla and 1.5 Tesla: Protocol optimization and application to cartilage, ligament and tendon pathology in cadaver specimens. Eur Radiol. 2007; 17(6): 1518–1528.
20. Lee KB, Bai LB, Park JG, et al. A comparison of arthroscopic and MRI findings in staging of osteochondral lesions of the talus. Knee Surg Sports Traumatol Arthrosc.2008;16(11): 1047-1051.
21. Hoelscher-Doht S, Frey1 S, Kiesel S, et al. Subtalar Dislocation: Long-Term Follow-Up and CT-Morphology. Open Journal of Orthopedics, 2015;5,53-59.
22. Gholami R, Alamdara S and Sadeghi R. Cuboid Fracture in a Toddler Discovered on the Whole Body Bone Scan: A Case Report. Iran J Nucl Med 2010;18(2):52-55.
23. Ansari MAQ. Isolated complete dislocation of the tarsal navicular without fracture: A rare injury. Ci Ji Yi Xue Za Zhi 2016;28(3):128-131.
24. Bica D, Sprouse A and Armen J (2016). Diagnosis and Management of Common Foot Fractures. American Family Physician 2016;93(3):183-191.
25. Bowes J and Buckley R. Fifth metatarsal fractures and current treatment. World J Orthop 2016; 18; 7(12): 793-800.
26. Khoury NJ, el-Khoury GY, Saltzman CL, Brandser EA. MR imaging of posterior tibial tendon dysfunction. AJR Am J Roentgenol. 1996 Sep;167(3):675-82.
27. Yousef H, Omar M and Kotb M. MRI Evaluation of Achilles Tendon Injuries. Med. J. Cairo Univ.2012; (80):195-200.
28. Chen TM, Rozen WM, PAN WR, Ashton MW, Richardson MD and Taylor G.I. The arterial anatomy of the Achilles tendon: Anatomical study and clinical implications. Clin. Anat., 22 (3): 377-385, 2009.
29. Molloy A and Wood E.V. Complications of the treatment of Achilles tendon ruptures. Foot Ankle Clin.,14 (4): 745-59, 2009.
30. Salvi AE, Metelli GP, Bosco A, Berizzi A, Hacking SA, Cantalamessa A. Spontaneous bilateral Achilles tendon rupture in a patient treated with oral levofloxacin. J Orthop Traumatol. 2007;8(2):86–90.
31. Schweitzer ME and Karasick D. MR imaging of disorders of the Achilles tendon. AJR 2000;175:613-625.

32. Wang XT, Rosenberg ZS, Mechlin MB, et al. Normal variants and diseases of the peroneal tendons and superior peroneal retinaculum: MR imaging features. Radio- Graphics 2005;25(3):587–602.
33. Taljanovic M, Alcala J, Gimber L, et al. High Resolution US and MR Imaging of Peroneal Tendon Injuries. RadioGraphics 2015;35:179-199.
34. Lee SJ, Jacobson JA, Kim SM, et al. Ultrasound and MRI of the peroneal tendons and associated pathology. Skeletal Radiol 2013;42(9):1191-1200.
35. O'Donnell P1, Saifuddin A. Cuboid oedema due to peroneus longustendinopathy: a report of four cases. Skeletal Radiol. 2005 Jul;34(7):381-8.
36. Lee M, Chung C, Cho J, et al. Tibialis Anterior Tendon and Extensor Retinaculum: Imaging in Cadavers and Patients with Tendon Tear. AJR 2006;187:161-168.
37. Gallo RA, Kolman BH, Daffner RH, Sciulli RL, Roberts CC, DeMeo PJ. MRI of tibialis anterior tendon rupture. Skeletal Radiol. 2004 Feb;33(2):102-6.
38. Conti SF, Michelson J and Jahss M. Clinical significance of magnetic resonance imaging in preoperative planning for reconstruction of posterior tibial tendon ruptures. Foot Ankle 1992; 13:208-214.
39. Oloff L and Schulhofer S. Flexorhallucislongus dysfunction. J Foot Ankle Surg 1998;37(2):101-109.
40. Komiya K and Terada N. Entrapment of the Flexor Hallucis Longus Tendon by Direct Impalement in the Osseofibrous Tunnel Under the Sustentaculum Tali: An Extremely Rare Complication of a Calcaneal Fracture: A Case Report. JBJS Case Connect. 2014 Oct/Dec/Nov;4(4): e100.
41. Larue B and Anctil E. Distal anatomical relationship of the flexor hallucislongus and flexor digitorumlongus tendons. Foot Ankle Int2006; (27):528-532.
42. Rosenberg ZS, Beltran J and Bencardino JT. MR imaging of the ankle and foot. RadioGraphics 2000;20:153-179.
43. Bencardino J, Rosenberg ZS, Delfaut E. MR imaging of sports injuries of the foot and ankle. MagnReson Imaging Clin N Am. 1999;7:131-49.
44. Nazarenko A, Beltran LS and Bencardino JT. Imaging evaluation of traumatic ligamentous injuries of the ankle and foot. RadiolClin North Am. 2013;51:455-478.
45. Gonzalez FM and Morrison WB. Magnetic resonance imaging of sports injuries involving the ankle. Top MagnReson Imaging. 2015;24:205-213.
46. Chhabra A, Subhawong TK and Carrino JA. MR imaging of deltoid ligament pathologic findings and associated impingement syndromes. Radiographics 2010;30:751-761.
47. Fallat L, Grimm DJ, Saracco JA. Sprained ankle syndrome: prevalence and analysis of 639 acute injuries. J Foot Ankle Surg. 1998;37:280-5.
48. Perrich K, Goodwin D, Hecht P, et al. Ankle Ligaments on MRI: Appearance of Normal and Injured Ligaments. AJR 2009;193:687-695.
49. Amendola A, Williams G, Foster D. Evidence-based approach to treatment of acute traumatic syndesmosis (high ankle) sprains. Sports Med Arthrosc. 2006;14:232-6.
50. Lektrakul N, Chung CB, Lai Ym, et al. Tarsal sinus: arthrographic, MR imaging, MR arthrographic, and pathologic findings in cadavers and retrospective study data in patients with sinus tarsi syndrome. Radiology. 2001;219:802-10.
51. Breitenseher MJ, Haller J, Kukla C, Gaebler C, Kaider A, Fleischmann D, et al. MRI of the sinus tarsi in acute ankle sprain injuries. J Comput Assist Tomogr. 1997;21:274-9.
52. Cerezal L, Abascal F, Canga A, et al. MR Imaging of Ankle Impingement Syndromes. AJR2002;181:551-559.
53. Illescas M, Rodríguez M, Pardo L, et al. MRI imaging of impingement syndromes of the ankle. ECR2015/C-1627:1-31.
54. Berman Z, Tafur M, Ahmed S, et al. Ankle impingement syndromes: an imaging review. Br J Radiol 2017; 90:1-14.
55. José A and Narvaez. March 2000 Radio Graphics, 20, 333-352.
56. Lawrence D, Rolen M, Abi Morshed K, et al. MRI of Heel Pain (2013). AJR 2013;200:845–855.
57. Cheng-Chang Lu, Yu-Min Cheng and Yin-Chih Fu. Angle Analysis of Haglund Syndrome and its Relationship with Osseous Variations and Achilles Tendon Calcification. Foot & Ankle International/Vol. 28, No. 2/February 2007.
58. Steenstra F and Van Dijk CN. The Achilles tendon: endoscopic techniques. London: Springer; 2007. P133-40.
59. Baghla DP, Shariff S and Dega R. Calcaneal osteomyelitis presenting with acute tarsal tunnel syndrome: a case report. J Med Case Reports 2010; 4: 66.
60. Ormeci T, Mahirogullar M and Aysal F. Tarsal tunnel syndrome masked by painful diabetic polyneuropathy. Int J Surg Case Rep. 2015; 15:103-106.
61. Lim PS, Schweitzer ME, Deely DM, Wapner KL, Hecht PJ, Treadwell JR, Ross MS, Kahn MD. Posteriortibial tendon dysfunction: secondary MR signs. Foot Ankle Int.1997 Oct;18(10):658-63.
62. Pineda C, Vargas A and Rodriguez AV. Imaging of osteomyelitis: current concepts [Systematic review or meta-analysis]. Clin North Am 2006;20 (4):789-825.
63. Canale ST, Beaty JH and Campbell WC. Campbell's operative orthopaedics. 12th edition. St Louis (MO); London: Mosby; 2012.

64. Wagner FW Jr. The diabetic foot [Systematic review or meta-analysis]. Orthopedics 1987;10(1):163-72.
65. Rathur HM and Boulton AJ. The neuropathic diabetic foot. Nat Clin Pract Endocrinol Metab 2007; 3:14-25.
66. Sanverdi SE, Ergen BF, Oznur A. Current challenges in imaging of the diabetic foot. Diabet Foot Ankle. 2012;3:10.
67. Schweitzer ME, Daffner RH, Weissman BN, et al. ACR Appropriateness Criteria on suspected osteomyelitis in patients with diabetes mellitus. J Am Coll Radiol2008;5(8):881-6.
68. Ledermann HP, Morrison WB, Schweitzer ME, et al. Tendon involvement in pedal infection: MR analysis of frequency, distribution, and spread of infection. AJR Am J Roentgenol2002;179: 939-947.
69. Donovan A and Schweitzer ME. Current concepts in imaging diabetic pedal osteomyelitis. Radiol Clin North Am 2008; 46(6):1105-1124.
70. Loredo R, Rahal A, Garcia G, et al. Imaging of the diabetic foot diagnostic dilemmas. Foot Ankle Spec 2010;3(5):249-264.
71. Ledermann HP, Morrison WB, Schweitzer ME, et al. Tendon involvement in pedal infection: MR analysis of frequency, distribution, and spread of infection. AJR Am J Roentgenol2002;179: 939-947.
72. Rajbhandari SM, Jenkins RC, Davies C, et al. Charcot neuroarthropathy in diabetes mellitus. Diabetologia 2002;45:1085-96.
73. Kapoor A, Page S, La Valley M, et al. Magnetic resonance imaging tor diagnosing foot osteomyelitis. Arch Intern Med 2007; 167: (2):125-132.
74. chatz J, Soper J, McCormack S, et al. Imaging of tumors in the ankle and foot. Top Magn Reson Imaging 2010;21:37-50.
75. Walker E, Michael E., Joel S and Murphey M (2011). Magnetic Resonance Imaging of Benign Soft Tissue Neoplasms in Adults. Radiol Clin N Am 2011; (49)1197-1217.
76. Steiner E, Steinbach LS, Schnarkowski P, Tirman PF, Genant HK (1996). Ganglia and cysts around joints. Radiol Clin North Am 34 (2):395–425.
77. Van Hul E, Vanhoenecker F, Van Dyck P, De Schepper A, Parizel PM. Pseudotumoral soft tissue lesions of the foot and ankle: a pictorial review. Insights Imaging 2011;2:439-452.
78. Robbin MR, Murphey MD, Temple HT, et al. Imaging of musculoskeletal fibromatosis. Radiographics 2001;21(3):585-600.
79. Wu KK (1996) Morton's interdigital neuroma: a clinical review of its etiology, treatment, and results. J Foot Ankle Surg 35(2):112–119
80. Zanetti M and Weishaupt D. MR imaging of the forefoot: Morton neuroma and differential diagnoses. Semin Musculoskelet Radiol 2005;9(3):175-186.
81. Singer AD, Datir A, Tresley J et al. Benign and malignant tumors of the foot and ankle. Skeletal Radiol 2016;45:287-305.
82. Bancroft LW, Peterson JJ, Kransdorf MJ. Imaging of soft tissue lesions of the foot and ankle. Radiol Clin North Am 2008;46:1093–1103.
83. Woertler K. Soft tissue masses in the foot and ankle: characteristics on MR imaging. Semin Musculoskelet Radiol 2005;9:227-242.
84. Foo LF and Raby N. Tumors and tumor-like lesions in the foot and ankle. Clin Radiol 2005;60:308-332.
85. Hochman MG and Wu JS. MR imaging of common soft tissue masses in the foot and ankle. Magn Reson Imaging Clin N Am 2017;25:159-181.
86. Boutry N, Flipo RM, Cotten A. MR imaging appearance of rheumatoid arthritis in the foot. Semin Musculoskelet Radiol 2005; 9 (3):199–209.
87. Sanders TG, Linares R, Su A. Rheumatoid nodule of the foot: MRI appearances mimicking an indeterminate soft tissue mass. Skeletal Radiol 1998;27:457-460.
88. Gollwitzer H, Toepfer A, Gerdesmeyer L, et al. Tumors and Tumor-Like Lesions of the Foot and Ankle: Diagnosis and Treatment. International Advances in Foot and Ankle Surgery 2014;10:489-508.
89. Tsang K, Chan W, Chan M, et al. Synovial Sarcoma: Epidemiology, Prognosis, and Imaging in a Tertiary Referral Centre. Hong Kong J Radiol. 2016;19:19-27.
90. Matushansky I, Charytonowicz E, Mills J, et al. MFH classification: differentiating undifferentiated pleomorphic sarcoma in the 21st century. Expert Rev Anticancer Ther. 2009;9(8):1135-1144.
91. Murphey MD, Arcara LK, Fanburg-Smith J. From the archives of the AFIP: imaging of musculoskeletal liposarcoma with radiologic-pathologic correlation. Radiographics. 2005;25(5):1371-1395.
92. Kuna S, Gudena R. "Soap bubble" in the calcaneus. CMAJ 2011;183:1171.
93. Kransdorf MJ and Sweet DE. Aneurysmal bone cyst: Concept, controversy, clinical presentation, and imaging. AJR Am J Roentgenol 1995;164:573-80.
94. Kaplanoğlu V, Ciliz DS, Kaplanoğlu H, Elverici E. Aneurysmal bone cyst of the calcaneus. J Clin Imaging Sci. 2014;4:60.

11/30/2019